Nucleic Acids Research, 1999, Vol. 27, No. 2 **403–410**

Detailed analysis of stem I and its 5′ and 3′ neighbor regions in the *trans*-acting HDV ribozyme

Fumiko Nishikawa, Mala Roy, Hamid Fauzi and Satoshi Nishikawa*

National Institute of Bioscience and Human Technology, AIST, MITI, 1-1 Higashi, Tsukuba Science City, Ibaraki 305-8566, Japan

Received July 24, 1998; Revised and Accepted November 13, 1998

ABSTRACT

To determine the stem I structure of the human hepatitis delta virus (HDV) ribozyme, which is related to the substrate sequence in the *trans*-acting system, we kinetically studied stem I length and sequences. Stem I extension from 7 to 8 or 9 bp caused a loss of activity and a low amount of active complex with 9 bp in the *trans*-acting system. In a previous report, we presented cleavage in a 6 bp stem I. The observed reaction rates indicate that the original 7 bp stem I is in the most favorable location for catalytic reaction among the possible 6–8 bp stems. To test base specificity, we replaced the original GC-rich sequence in stem I with AU-rich sequences containing six AU or UA base pairs with the natural +1G·U wobble base pair at the cleavage site. The *cis*-acting AU-rich molecules demonstrated similar catalytic activity to that of the wild-type. In *trans*-acting molecules, due to stem I instability, reaction efficiency strongly depended on the concentration of the ribozyme–substrate complex and reaction temperature. Multiple turnover was observed at 37°C, strongly suggesting that stem I has no base specificity and more efficient activity can be expected under multiple turnover conditions by substituting several UA or AU base pairs into stem I. We also studied the substrate damaging sequences linked to both ends of stem I for its development in therapeutic applications and confirmed the functions of the unique structure.

INTRODUCTION

The genome of the human hepatitis delta virus (HDV) is a single-stranded circular RNA of ~1700 nt, which apparently replicates through a rolling circle RNA to RNA pathway, as do some plant pathogenic RNA viruses (1–4). Both genomic and antigenomic HDV RNAs have self-cleavage activity (i.e. are ribozymes) in the presence of divalent metal ions, producing a 2′,3′-cyclic phosphate and 5′-OH group (1,2), as do hammerhead, hairpin and *Neurospora* VS ribozymes. The primary sequence does not resemble these ribozymes and the details of the reaction mechanism remain unknown.

Several models of the secondary structure have been proposed for genomic and antigenomic HDV ribozymes and many attempts have been made to clarify the roles of different bases and to define the structure of the catalytic core of the HDV ribozyme (reviewed in 5,6). The pseudoknot secondary structure is well supported by many experimental results and designed *trans*-acting systems have provided confirmation. This pseudoknot structure consists of two stems (I and II), two stem–loops (III and IV) and three single-stranded regions (SSrA, B and C in Fig. 1) in both genomic and antigenomic *cis*-and *trans*-acting ribozymes (7–11). The structure was also recently suggested to exist and function *in vivo* (12). In the pseudoknot model, stem I, originally consisting of 7 bp, forms a cleavage site at the 5′-end, stems II and III retain the catalytic core structure and stem IV is related to the backbone that stabilizes the structure (Fig. 1). We recently clarified that ribozyme activity is retained without stem IV (13).

In the *trans*-acting system divided at junction I–II (5,10,14,15), stem I is separated by a substrate and ribozyme portion. In this study, we focused on stem I (recognition site for ribozyme, target sequence) and kinetically studied its optimal length and base specificity. We found that the length of 7 bp in the natural stem I lies in most efficient proximity to the catalytic core and the result of inserting an AU-rich sequence in stem I suggests no base specificity except for the critical +1 position adjacent to the cleavage site (the +1G·U725 wobble base pair is the most preferable). To learn more, we investigated neighbor bases linked to both ends of stem I, which interfere with the functional structure of SSrA and stem III.

MATERIALS AND METHODS

Substrate and ribozyme synthesis

All oligonucleotides were synthesized using an automated DNA/RNA synthesizer (model 392 or 394; Applied Biosystems). DNA and RNA phosphoramidites were purchased from Glen Research. Products were purified as described in the user bulletin from ABI (no. 53, 1989) with minor modifications.

Substrate sequences (S1, +8GS1, rev. S1, +1Crev. S1, 6US1, 6AS1, –1CS1, S2, S3C/U, S4, S5 and R10) were as follows: S1, 5′-GAUGGCCGGCAUG-3′; +8GS1, 5′-GAUGGCCGGC-GUG-3′; rev. S1, 5′-GAUUCGGCCGAUG-3′; +1Crev. S1, 5′-GAUCCGGCCGAUG-3′; 6US1, 5′-GAUGUUUUUUA-

*To whom correspondence should be addressed. Tel: +81 298 54 6085; Fax: +81 298 54 6095; Email: nisikawa@nibh.go.jp

UG-3′; 6AS1, 5′-GAUGAAAAAAAUG-3′; –1CS1, 5′-GACGGCCGGCAUG-3′; S2, 5′-CCGGCCGGC-3′; S3C/U, 5′-CCC/UGGCCGGC-3′; S4, 5′-GAUGGCCGGCGC-3′; S5, 5′-GAUGGCCGGCGCC-3′; R10, 5′-GAUGGCCGGC-3′ (stem I regions are underlined).

All ribozymes were prepared by run-off transcription (AmpliScribe T7 transcription kit; Epicentre Technologies) of the appropriate plasmids after digestion with *Bam*HI or, for TdS4(Xho) only, *Xba*I and purified on 8% polyacrylamide denaturing gels containing 7 M urea.

Construction of modified *trans*-acting ribozymes of TdS4(Xho) and *cis*-acting ribozymes

The *trans*-acting ribozymes TdS4(Xho) and TdS4 and the *cis*-acting ribozyme CdS4 were constructed as described elsewhere (13,16). Vectors containing the sequences of modified ribozymes were prepared using a system for oligonucleotide-directed *in vitro* mutagenesis (Amersham) after isolation of the proper single-stranded DNA. The following mutated primer sequences were used (mutated bases are underlined, a dash means a deletion site): primer Rz1, d[5′-CCCAGCCGGCGGCCAGCGAGG-3′]; primer Rz2, d[5′-CCCAGCCGGCGTGCCAGCGAGG-3′]; primer Rz3, d[5′-AATGTTGCCCCCGGCCGGCCAGCGAGG-3′]; primer Rz4, d[5′-AATGTTGCCCATTTTTTGCCAGCGAGG-3′]; primer Rz5, d[5′-AATGTTGCCCAAAAAAAGCCAGCGAGG-3′]; primer TdS4, d[5′-GAGGCTGGGA-CCTATAGTGA-3′]; primer *cis*-6UA, d[5′-AATGTTGCCCATTTTTTGCCAGCGAGGAGGCTGGGACCATAAAAAAACATCAGGCTCG-3′]; primer *cis*-6AU, d[5′-AATGTTGCCCAAAAAAAGCCAGCGAGGAGGCTGGGACCATTTTTTTCATCAGGCTCG-3′].

Cloning and vectors

Vector pUCT7 was a modified version of pUC118; it included the promoter for T7 RNA polymerase and a *Xho*I site (not for TdS4) at the *Eco*RI–*Bam*HI site (17). All experiments were conducted with *Escherichia coli* MV1184 as the host. Plasmid DNA was prepared from an overnight culture and purified with Qiagen-tip 20 (Qiagen). DNA sequencing was conducted using double-stranded DNA as a template on a DNA sequencer (Model 373A; Applied Biosystems) and a Taq DyeDeoxy Terminator Cycle Sequencing Kit (Applied Biosystems).

Trans-acting ribozyme cleavage

The 5′-end of each substrate was labeled with [γ-^{32}P]ATP by T4 polynucleotide kinase (Takara). The cleavage reaction was conducted under ribozyme saturating (single turnover) conditions as follows: 5 or 10 µM ribozyme, 0.01 µM substrate, 10 mM Mg^{2+} in 50 mM Tris–HCl (pH 7.4) at 37°C. The reaction solution containing the ribozyme and substrate in Tris–HCl without $MgCl_2$ was denatured at 90°C for 2 min and cooled on ice. The solution was then incubated at 37°C for 10 min and the reaction was initiated by adding $MgCl_2$ solution. At appropriate times, aliquots of the reaction mixture were removed and the reaction was stopped by adding an equal volume of stop solution (9 M urea, 50 mM EDTA, 0.1% bromophenol blue and 0.1% xylene cyanol) on ice. After electrophoretic fractionation on 20% polyacrylamide gels containing 7 M urea, the substrate and cleaved product on the gel were determined using a bioimaging analyzer (BAS2000; Fuji Film).

Cleavage activity was indicated by the rate at which the cleaved product formed. For kinetic analysis, we used a simple pseudo-first-order equation, cleaved yield (%) = $[EP]\cdot(1 - e^{-kt})$ (Table 1), and fitted the experimental data to a curve (16,18,19). This assumes that under excess ribozyme conditions, substrates were saturated with the ribozyme at time 0. This analysis procedure is the same as the self-cleavage reaction of the *cis*-acting HDV ribozyme reported by Been *et al*. (15). Thus, substrate cleavage proceeds as a first-order reaction. The cleavage reaction consists of two steps, i.e. a conformational change and a chemical reaction. From our kinetic analysis, we cannot conclude that k_{obs} reflects either the conformational change or chemical step.

A cleavage reaction under multiple turnover was conducted with the following substrate excess conditions: 1 µM ribozyme, 3–80 µM substrate, 10 mM Mg^{2+} in 50 mM Tris–HCl [pH 6.26 for 6UA and 6AU, pH 7.4 for TdS4(Xho)/Bam] at 25 or 37°C. The reaction was followed as described for single turnover conditions.

Preparation of *cis*-acting ribozyme and cleavage activity

Plasmid DNA linearized with *Bam*HI was used for transcription *in vitro*. The reaction mixture (30 µl) for transcription contained 40 mM Tris–HCl (pH 8.0), 8 mM $MgCl_2$, 2 mM spermidine, 5 mM dithiothreitol, ribonucleotides at 2 mM each, 0.5 mCi/ml [α-^{32}P]CTP, 3 µg of linear plasmid DNA and 150 U T7 RNA polymerase (Takara). After 30–60 min at 37°C, an equal volume of stop solution was added and the mixture was heat denatured and fractionated by electrophoresis on 8% polyacrylamide gels containing 7 M urea. The transcript RNA was located by autoradiography and the uncleaved precursor RNA was excised from the gel, extracted with 0.1 mM EDTA and 0.3 M NaOAc and recovered by ethanol precipitation. Cleavage reactions containing ~5–50 nM RNA were conducted in 50 mM Tris–HCl (pH 7.4) and 10 mM $MgCl_2$ at 25 and 37°C. The labeled *cis*-acting ribozyme in 50 mM Tris–HCl (pH 7.4) was denatured at 90°C for 2 min, slowly cooled down over 1 h and preincubated at 25 or 37°C for 10 min. Reaction was started by adding prewarmed $MgCl_2$ solution. Aliquots were taken at appropriate times and followed in the same way as the *trans*-cleavage reaction. The cleaved fraction was calculated as $(counts_{3'\text{-product}})/(counts_{precursor} + counts_{3'\text{-product}})$. The first-order rate constant (k) and end point (EP) were obtained by fitting data to the equation: cleaved yield (%) = $[EP]\cdot(1 - e^{-kt})$.

RESULTS AND DISCUSSION

Extension of stem I base pairs

Wu *et al*. reported that in the *cis*-acting genomic HDV ribozyme extending or shortening of stem I by 2 bp lost catalytic activity (20). To better characterize stem I and improve activity, we tested the effect of stem I extension in the *trans*-acting genomic HDV ribozyme. Inserting U between C718 and G719 to extend stem I can result in two possibilities, a 1 bp extension of stem I or another base pair with 704A (Fig. 1). To prevent analytical ambiguity, we replaced position +8A in substrate S1 with +8G (+8GS1). We also inserted one C nucleotide or the dinucleotide 5′-AC-3′ between C718 and G719 of the *trans*-acting ribozyme TdS4(Xho) and designated these ribozymes Rz1 and Rz2 (Fig. 2B and C). Inserting these additional nucleotides may change the conformation of the ribozyme even though the original 7 bp are held in stem I.

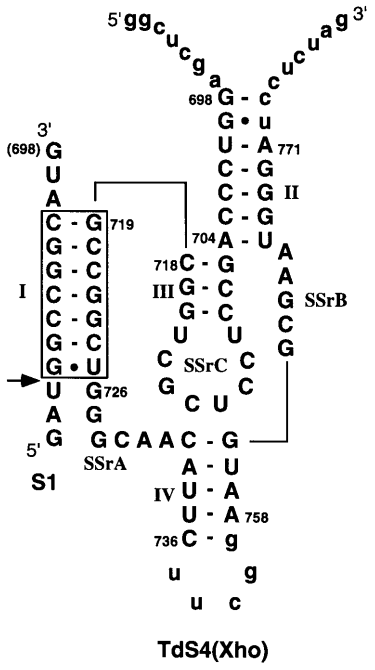

Figure 1. Secondary structure of *trans*-acting genomic HDV ribozyme TdS4(Xho). Numbering is based on that of Makino *et al.* (35). Lower case letters in 5′- and 3′-sequences indicate vector-derived sequences. Single-stranded regions are marked SSrA (726–731), SSrB (762–766) and SSrC (708–715) as reported previously (8,29). To truncate the original stem IV, a wild-type sequence from nt 736 to 758 was changed to include a uucgg sequence. An arrow indicates the cleavage site. The original stem I sequence is shown in the rectangle.

Accordingly, as a control, we conducted the same experiments with a short substrate R10, which has only 7 bp at stem I with the ribozyme (Fig. 2D–F). The experimental data are summarized in Table 1.

Table 1. Comparison of cleavage efficiencies on extension of stem I

Substrate \ Rz	TdS4(Xho) k_{obs} (min^{-1})	TdS4(Xho) EP (%)	Rz1 k_{obs} (min^{-1})	Rz1 EP (%)	Rz2 k_{obs} (min^{-1})	Rz2 EP (%)
S1	(A) 1.90	77				
+8GS1	0.315	74	(B) 0.053	50	(C) 0.039	5
R10	(D) 2.17	93	(E) 0.062	35 [57]	(F) 0.107	38 [64]

Ribozymes, TdS4(Xho), Rz1 and Rz2; substrates, +8GS1 and R10. *Trans* cleavage reactions were conducted under standard conditions (Materials and Methods) at least twice. Kinetic parameters (k_{obs} and EP) show the average of each fitting. Values in brackets show the cleavage percentage after 2 h. The kinetic parameters of E and F were determined by fitting to the equation at 30 min. The error of the mean does not exceed 15%.

A 1 bp extension in stem I (Fig. 2B) caused a 6-fold decrease in catalytic activity (k_{obs} = 0.053/min, EP = 50%) compared with 8GS1 (7 bp) and the control (Fig. 2E) showed similar values (k_{obs} = 0.062/min, 57% cleaved after 2 h). This suggests that the activity of Rz1 is not lost due to the 1 bp extension of stem I but due to the 1 nt insertion between 718C and 719G of the ribozyme. We also studied the effect of a U instead of C insertion in the 8 bp molecule in Figure 2B, obtaining k_{obs} = 0.014/min and EP = 46%. The greater k_{obs} decrease suggested some interaction between

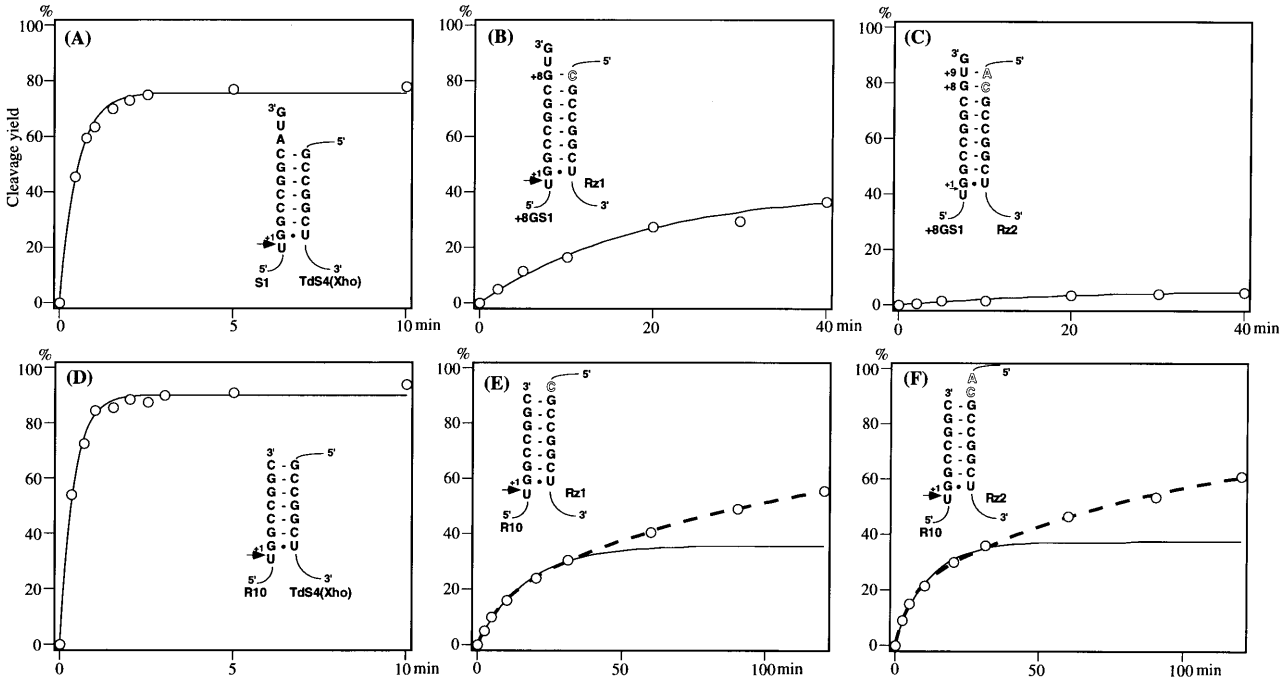

Figure 2. Effect of extension of base pairs in stem I in *trans*-acting genomic HDV ribozyme. Cleavage reactions were conducted under standard conditions. Data points were fitted to a pseudo-first-order equation (continuous lines; Materials and Methods) or biphasic first-order equation (broken lines; Results and Discussion). Outlined letters indicate inserted nucleotides. (**A**) Original 7 bp stem I, substrate S1 versus *trans*-acting ribozyme TdS4(Xho); (**B**) 8 bp stem I, substrate +8GS1 versus Rz1; (**C**) 9 bp stem I, +8GS1 versus Rz2; (**D**) R10 versus TdS4(Xho); (**E**) R10 versus Rz1; (**F**) R10 versus Rz2.

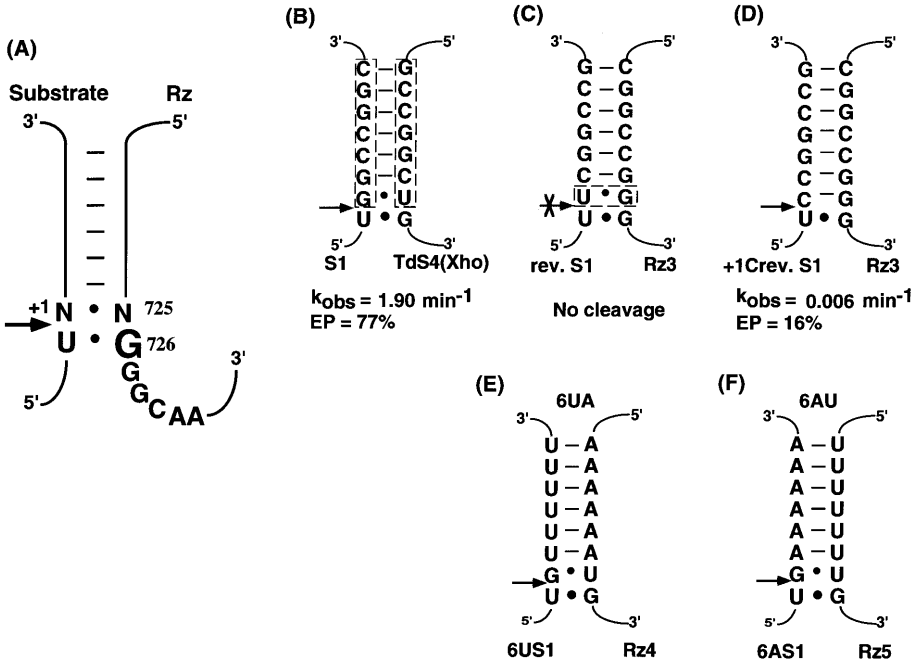

Figure 3. Cleavage reactions with different stem I sequences in the *trans*-acting system. Kinetic data were obtained from a pseudo-first-order equation. (**A**) Stem I and SSrA; (**B**) original stem I sequence, substrate S1 versus *trans*-acting ribozyme TdS4(Xho); (**C**) interchanged stem I, rev. S1 versus Rz3; (**D**) Substitution of +1U for C of interchanged stem I, +1C rev. S1 versus Rz3; (**E**) AU-rich stem I, 6UA, 6US1 versus Rz4; (**F**) 6AU, 6AS1 versus Rz5.

704A and the inserted U, but it is not clear whether this was due to nucleotide insertion, interaction with 704A or stem III extension. In the 9 bp stem I (Fig. 2C), the observed reaction rate (k_{obs}) was almost the same as for 8 bp (Table 1B and C) but the amount of active complex markedly decreased (EP = 5%). In contrast, the 2 nt insertion control (Fig. 2F and Table 1F) did not show decreases in either k_{obs} or EP, although some increase in k_{obs} was observed.

In the control reactions, data points closely fitted the equation, showing a monophasic reaction (Materials and Methods) up to 30 min; thereafter, data points of cleavage percentage obviously deviated from the fitting curve (Fig. 2E and F). Cleavage yields after 2 h were added to Table 1E and F, assuming a slower reacting molecule as another reaction component and using the following equation: cleaved yield (%) = $[EP_1]\cdot(1-e^{-k_1 t}) + [EP_2]\cdot(1-e^{-k_2 t})$. The results were in good agreement (Fig. 2E and F, broken lines). The slower reaction dominates the faster one in the ratio 3–4:1 and the calculated major slower reaction rate was 0.012/min. The average k_1 and k_2 values are close to the k_{obs} determined from the data points up to 30 min using a monophasic equation (Table 1E and F). This result indicates that these HDV ribozyme variants are not uniform in structure but contain some misfolding.

We reported that one HDV ribozyme variant shifted the cleavage site 1 nt toward the 3′-end and 6 bp in stem I are sufficient for cleavage (18). It is thus possible to cleave within the 6–8 bp stem I, while the 9 bp stem I is distant from the essential bases in SSrB (nt 762–766) and SSrC (708–715) which form the catalytic core with essential bases in SSrA (726–731) (8,17). Comparing all observed reaction rates, the natural 7 bp stem I showed the highest value and is located in the most favorable position to construct a catalytic core.

Stem I base specificity

From the many results of mutagenesis at several positions in stem I, it has been accepted that base pairing is required and the complementary substitution of base pairs can restore catalytic activity (7,15,21,22). In addition, we recently identified 726G as the only essential base in the cleavage site (Fig. 3A; 18). To verify the sequence specificity of the HDV ribozyme (Fig. 3B), we first interchanged the sequences of the substrate and ribozyme forming stem I (rev. S1 and Rz3) and checked the catalytic activity (Fig. 3C). Interchanging stem I with +1U·G725 resulted in no production of cleaved product after 1 h. When +1U was substituted for C (+1C·G725, Fig.3D), however, catalytic activity recovered (k_{obs} = 0.006/min, EP = 16%). In addition to the previous mutagenesis results (7,15,21,22), it appears that no sequence specificity exists in the HDV ribozyme except for the essential 5′-end base pair in stem I.

For the +1N·N725 base pair (Fig. 3A), the G·U wobble pair has already been defined as the most efficient for cleavage and U·G is completely inactive (18,20,23). It is not yet clear why the +1 base pair contributes to catalytic activity, but recent X-ray crystallographic analysis of the RNA duplex with adjacent G·U and U·G pairs provides valuable information (24,25). The RNA duplex is slightly distorted in the presence of two adjacent U·G pairs (5′-UG-3′/3′-GU-5′, as in Fig. 3B) located at the center of the helix. The U·G pairs are bridged by water molecules and solvated in grooves. The twist angle between the wobble base pairs exceeds the average value and is stabilized by stacking two G bases (24) (i.e. 726G and +1G, Fig. 3A). Based on this X-ray crystallographic data, we can speculate that the metal ion binds

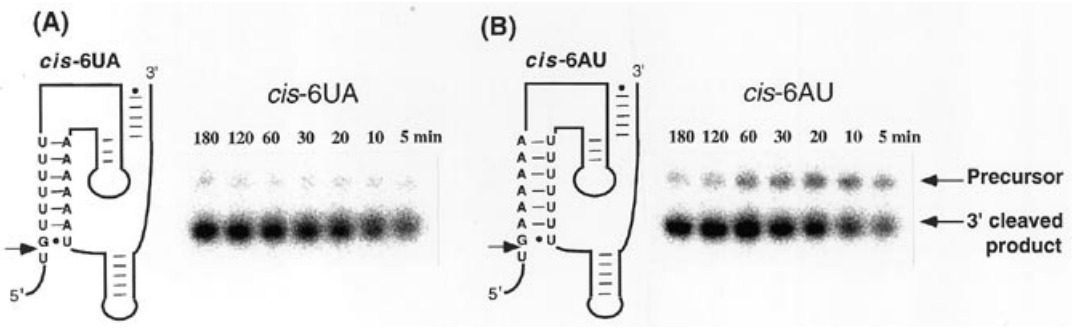

Figure 4. Cleavage reactions of mutant *cis*-acting HDV ribozymes with an AU-rich stem I, *cis*-6UA and *cis*-6AU. Cleavage patterns during *cis*-6UA (**A**) and *cis*-6AU (**B**) transcription, analyzed by 8% PAGE containing 7 M urea.

with nucleophile 2′-OH or *Rp* oxygen of the cleavage site directly or indirectly via water. The structure of the remaining combination (5′-UU-3′/3′-GG-5′) in this series, related to the inactive form +1U·G725 in the HDV ribozyme, requires further clarification of the structure around the cleavage site.

We then examined this expected loose base specificity by changing the original GC-rich sequence to an AU-rich stem I containing six UA (Fig. 3E) or AU (Fig. 3F) base pairs holding only one original +1G·U725 base pair at the cleavage site. In the *cis*-acting HDV ribozyme with the AU-rich stem I, cleavage quickly occurred and this self-cleavage reaction was observed even during transcription (8 mM Mg^{2+} in buffer) to prepare RNA, just as with the wild-type. During transcription, >95% of *cis*-6UA was cleaved within 5 min while slower *cis*-6AU took 3 h for almost total cleavage (Fig. 4A and B). The kinetic parameters of the cleavage reaction (Table 2) were determined with a biphasic reaction equation using isolated precursors on polyacrylamide gels. The faster reaction is dominant but 20–30% of the slower reaction is present in both cases. The rate of cleavage (k_{obs}) of *cis*-6UA is faster than that of *cis*-6AU. Secondary structure modeling by the Mulfold program (26) implies that *cis*-6AU assumes an unfavorable structure compared with *cis*-6UA (data not shown). This is probably the reason for the difference in k_{obs} between the two AU-rich molecules.

Table 2. *cis*-6UA and *cis*-6AU kinetic parameters

cis Rz	Temp. (°C)	k_1 (min^{-1})	k_2 (min^{-1})	EP_1 (%)	EP_2 (%)
cis-6UA	25	5.83 ± 0.06	0.14 ± 0.07	42	13
	37	6.39 ± 1.78	0.15 ± 0.18	43	9
cis-6AU	25	1.90 ± 0.20	0.21 ± 0.03	63	24
	37	2.88 ± 0.32	0.25 ± 0.10	57	22

The cleavage reaction was conducted under the following conditions: 10 mM Mg^{2+}, 40 mM Tris–HCl, pH 7.4, for *cis*-6UA and *cis*-6AU. Kinetic parameters were calculated from the arbitrary assumed biphasic first-order equation as a trial; cleaved yield (%) = $[EP_1]\bullet(1 - e^{-k1t}) + [EP_2]\cdot(1\text{-}e^{-k2t})$. Kinetic parameters indicate an average of at least two experimental data points (k_1 error does not exceed 11% or k_2 error 75%).

In *trans*-acting systems with the AU-rich stem I, cleavage was not observed under the standard conditions (single turnover, 5 µM Rz, 0.01 µM substrate, 10 mM Mg^{2+} at 37°C). This is probably due to the unstable AU-rich duplex compared with the GC-rich wild-type sequence and the cleavage reaction depends on the concentration of the ribozyme–substrate complex and reaction temperature. Cleavage was more efficient at lower temperatures (25 > 30 > 37°C; data not shown) and with higher concentrations of ribozyme/substrate (1 µM Rz, 0.01–80 µM substrate) than under the usual conditions. The cleavage reaction was conducted around the optimal pH 6.2–6.5. This variant ribozyme operated under multiple turnover conditions, although the reaction was very slow (>1 day; Fig. 5A). The cleavage reaction rate constants under steady-state were measured at several substrate concentrations and kinetic parameters were determined by an Eadie–Hofstee plot, which generates K_m (slope) and k_{cat} (*y*-intercept) (Fig. 5B, C, E and F) for 6UA (K_m = 38.6 µM, k_{cat} = 0.867/h, k_{cat}/K_m = 2.25 × 10^4/M/h) and for 6AU (K_m = 66.3 µM, k_{cat} = 0.528/h, k_{cat}/K_m = 7.96 × 10^3/M/h). In comparison with other *trans*-acting HDV ribozymes, RNA-37 retained the GC-rich antigenomic stem I sequence and the multiple turnover reaction occurred only at higher reaction temperatures, 50°C (K_m = 57 nM, k_{cat} = 0.66/min, k_{cat}/K_m = 1.1 × 10^7/M/h) (11). However, in the case of the AU-rich stem I, multiple turnover occurred at room temperature and also at 37°C (data not shown).

In contrast, a fast *trans*-acting genomic HDV ribozyme with wild-type stem I, TdS4(Xho), did not turn over at 37°C under the same conditions as for 6UA and 6AU. At 50°C, it could turn over but a burst was observed (Fig. 5D). The first round of reaction is very fast and the burst count indicated 1.03. These results indicate that there is no base specificity in stem I and more efficient activity can be expected under multiple turnover conditions by introducing several AU base pairs instead of the original base pairs into stem I. In our investigation of stem I base specificity of another HDV variant, CDC200 (15), which has a hybrid antigenomic and genomic sequence, the AU-rich stem I worked in multiple turnover at ambient temperature (data not shown). We also studied the same *cis* and *trans* reaction with other metal ions, such as Mn^{2+} and Ca^{2+}; Mg^{2+} ions showed the highest reaction activity (data not shown).

Ananvoranich and Perreault recently reported the substrate specificity of the antigenomic HDV ribozyme by introducing a mismatch in stem I (27). They show that the nucleotides in the middle of stem I are essential for substrate binding and subsequent steps in the cleavage pathway. Reduction or loss of cleavage activity by mismatch in stem I agrees with our results for the genomic HDV ribozyme. In other words, the formation of stem I is important for catalytic activity. Our phosphorothioate modification interference analysis suggests that stem I phosphates

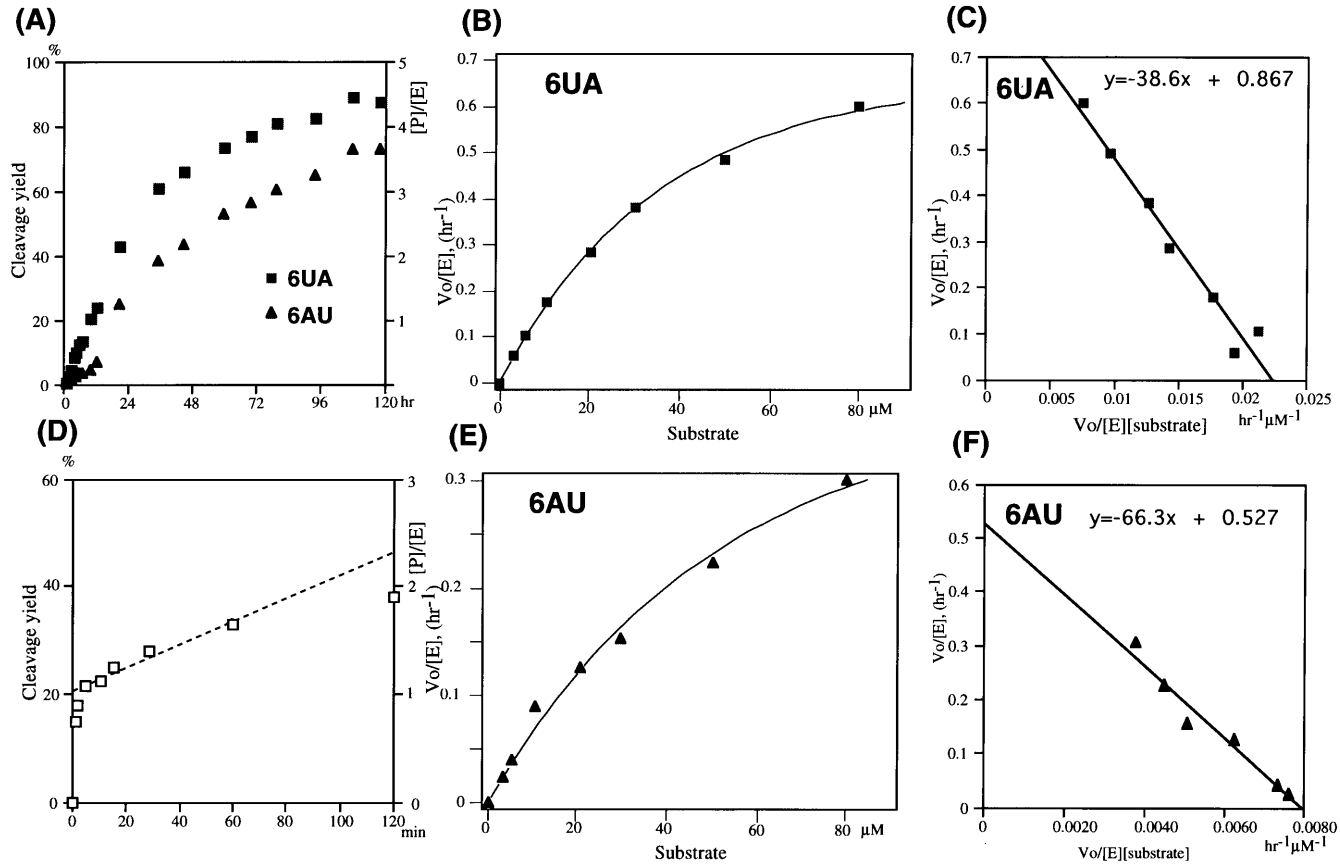

Figure 5. Cleavage reactions of *trans*-acting 6UA and 6AU under multiple turnover. (**A**) Time courses of cleavage reactions of 6UA and 6AU. Cleavage yield (left) and product generated per ribozyme ([P]/[E]) (right) are plotted as a function of time. [Rz], 1 μM (Rz4 or Rz5); [substrate], 5 μM (6US1 or 6AS1) for 6UA (solid squares) and 6AU (solid triangles); [Mg^{2+}], 10 mM, 40 mM Tris–HCl, pH 6.26, at 25°C. (**B** and **E**) Multiple turnover kinetics of 6UA and 6AU cleavage reactions. Cleavage was at different substrate concentrations (3–80 μM) and 1 μM ribozyme. The steady-state rate of cleavage (V_o, μM/h) was divided by the ribozyme concentration ([E], 1 μM) and V_o/[E] (per h) is plotted versus substrate concentration. (**C** and **F**) Eadie–Hofstee plot of data to generate K_m (slope) and k_{cat} (*y*-intercept), $y = -38.6x + 0.867$ for 6UA (C), $y = -66.3x + 0.527$ for 6AU (F). (**D**) Cleavage reaction with excess S1 using TdS4(Xho)/Bam. [P]/[E] is plotted as a function of time. The concentrations of ribozyme, substrate and Mg^{2+} are the same as for (A) in 40 mM Tris–HCl, pH 7.4, at 50°C. The line is fitted to the initial portion of the steady-state region of the time course. $y = 0.011x + 1.03$, slope = 0.011 ± 0.001/min and *y*-intercept = 1.03 ± 0.03 [P]/[E].

have some interactions with metal ions and/or other sites (28). These interactions may change duplex structure by nucleotide substitution in the middle of stem I. However, no conclusion about such tertiary interactions can be derived from this study.

Effect of 5′-side sequence at cleavage site on catalytic activity

In general, one 5′-side nucleotide at the substrate cleavage site is sufficient for catalytic activity in both genomic and antigenomic HDV ribozymes (7). For the –1 position (–1N·N726), we showed that G726 is essential and the –1N position can accept any base but shows a preference in the order U > A > C > G (18). The *trans*-acting HDV ribozyme, for example, could cleave at next to the initiation codon AUG (data not shown). In targeting other long RNA substrates, it is necessary to confirm the absence of the 5′ interfering sequence at the cleavage site. We clarified that, for its counterpart ribozyme, 726G and 727G in SSrA are essential, especially 726G in the genomic ribozyme (29), and three G residues are important in the antigenomic ribozyme (23).

First, we tested cleavage activity using an R10 analog able to hybridize with important G residues of SSrA. Substrate S2, which hybridizes with the important 726G727G (S2) (Fig. 6), decreased k_{obs} 80-fold from R10 by a further 2 bp extension of stem I. On a polyacrylamide gel containing 7 M urea, substrate S2 appeared as a tailing band (Fig. 6C), indicating that S2 hybridizes more strongly to the ribozyme than does R10. When SSrA was further masked with substrate S3C, cleavage was no longer detected (Fig. 6D). Even with a suitable –1U·G726 wobble base pair (Fig. 6E), the S3U substrate decreased catalytic activity 217 times (k_{obs} = 0.01/min, EP = 76%) below R10. Consequently, 5′-CCN-3′ (especially N = C) linked 5′ of the cleavage site sequence should be excluded from the target sequence. Masking important G residues of SSrA alters the structure of the substrate–ribozyme complex and interrupts formation of the catalytic core with other functions of SSrB and SSrC. 726G and 727G interact with the catalytic core directly or indirectly.

Effect of stem I 3′-side sequence on catalytic activity

An 8 nt substrate is the minimum substrate for efficient cleavage activity. One ribonucleotide is 5′ of the cleavage site and the rest form the 7 bp of stem I. The region linked 3′ of stem I does not play a role in the cleavage reaction. However, as mentioned above, for targeting long substrate RNA it is also important to

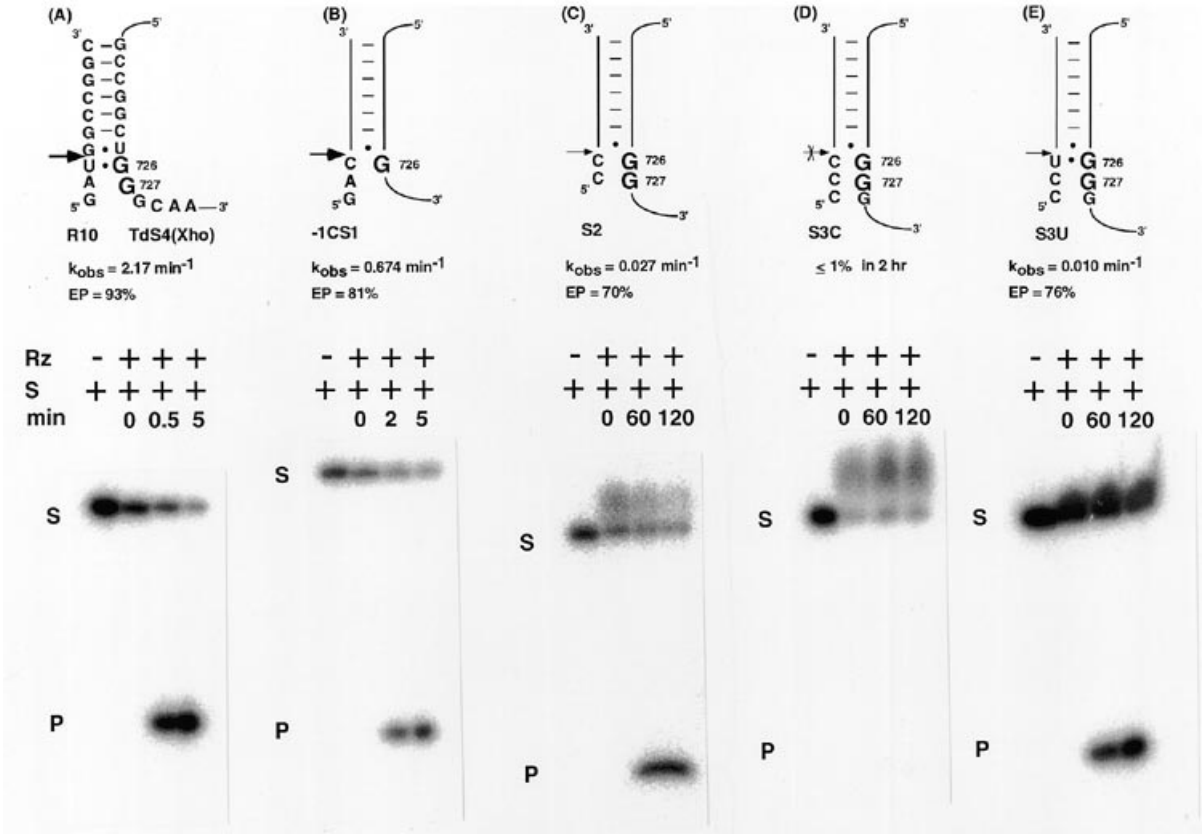

Figure 6. Effect of substrate 5′-part at the cleavage site on catalytic activity. *Trans* cleavage reactions were conducted under standard conditions (Materials and Methods) using TdS4(Xho) and different substrates and analyzed by denaturing PAGE. S, substrate; P, cleaved product. Kinetic values were obtained from pseudo-first-order equations. (**A**) Substrate R10; (**B**) –1CS1; (**C**) S2; (**D**) S3C; (**E**) S3U.

know whether some interfering sequence (from +8) adjacent to the 3′-end of stem I exists or not.

To determine the effect of this sequence, we tested cleavage activity using several substrates having extra sequences at the 3′-end that might disrupt stem III, the counterpart of the substrate, by forming base pairs (Fig. 7). Results indicate that k_{obs} decreased but EP did not change on increasing the number of probable interacting nucleotides (Fig. 7, outlined letters). This kinetic data suggests that the 3′-side of the substrate interacts with the stem III sequence. From the electrophoresis gel pattern, substrate S5 was observed as a weak tailing band and some interactions with ribozyme other than S1 and R10 were suspected (data not shown). In comparison with S3C (Fig. 6D), which halts ribozyme activity by blocking three G residues, the amount of active complex (EP = 73%) did not change dramatically and only k_{obs} decreased, reflecting the rate-limiting step of conformational change from an unfavorable to an active form. In stem III, restoring base pairs by compensatory changes revives activity and a mismatch causes low or no detectable activity (30). Accordingly, +8GCC (S5) interferes with the formation of stem III but does not disrupt stem III completely.

The central hairpin structure (stem III and SSrC) in antigenomic HDV ribozyme was recently elucidated by high resolution NMR spectroscopy by two groups (31,32). Although their results show some differences in loop structure, they both agree that the pyrimidine base pair between the 5′- and 3′-end nucleotides in the loop exists and stacks on stem III. In the genomic HDV ribozyme, the loop size is one base larger than the antigenomic one, but a similar pyrimidine base pair is expected in the loop (SSrC). In three-dimensional models of the tertiary structure of both genomic and antigenomic HDV ribozymes, stem III stacks on stem II coaxially (9,31). These data suggest that the three stem III base pairs are rather stable, with stacking of stem II and the pyrimidine base pair at the end of the loop.

CONCLUSIONS

We characterized stem I of the HDV ribozyme and its flanking sequences on both sides in a *trans*-acting system. These are summarized as follows: (i) in stem I, no base specificity except the critical +1 base pair is observed; (ii) the favorable 7 bp stem I among possible 6–8 bp stems is required to construct the catalytic core; (iii) multiple turnover in the reaction is possible with an AU-rich sequence of stem I at room temperature; (iv) CCC attached 5′ of the cleavage site almost completely diminishes cleavage activity; (v) an extra sequence complementary to GCC in stem III decreases catalytic activity; (vi) stem III is stable in the pseudoknot structure.

Recent X-ray crystallographic analysis of the 3′-product of the HDV ribozyme shows a very tight compact RNA folding (34). Extension of the base pairs or length of stem I seems to destroy

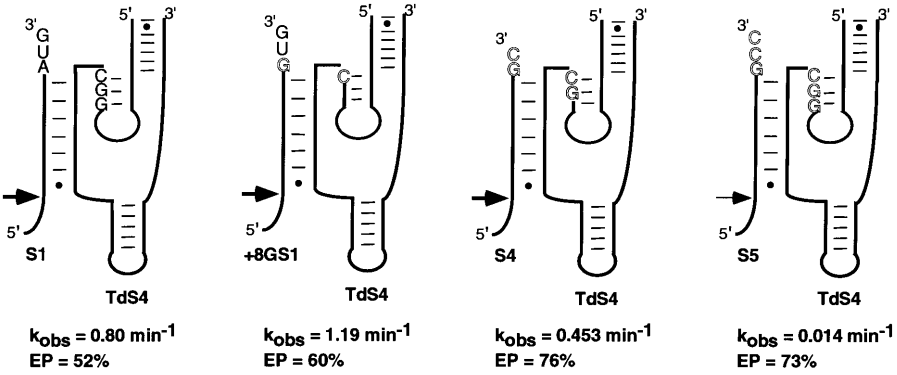

Figure 7. Effect of 3′-side sequence of substrate that may interact with stem III for catalytic activity. *Trans* cleavage reactions were conducted under standard conditions (Materials and Methods) using S1 substrate derivatives (S1, +8GS1, S4 and S5) with TdS4. TdS4 is a *trans*-acting ribozyme shortened by deleting restriction enzyme region *Xho*I from the 5′-end and *Xba*I from the 3′-end of TdS4(Xho). Outlined letters indicate possible interacting bases.

this compact folding structure and subsequently decreases its cleavage activity.

ACKNOWLEDGEMENT

We thank Dr Penmetcha Kumar for his comments on the manuscript.

REFERENCES

1 Kuo,M.Y.P., Sharmeen,L., Dinter-Gottlieb,G. and Taylor,J. (1988) *J. Virol.*, **62**, 4439–4444.
2 Sharmeen,L., Kuo,M.Y.P., Dinter-Gottlieb,G. and Taylor,J. (1988) *J. Virol.*, **62**, 2674–2679.
3 Wu,H.N., Lin,Y.J., Lin,F.P., Makino,S., Chang,M.F. and Lai,M.M.C. (1989) *Proc. Natl Acad. Sci. USA*, **86**, 1831–1835.
4 Lazinski,D.W. and Taylor,J.M. (1995) *RNA*, **1**, 225–233.
5 Been,M.D. and Wickham,G.S. (1997) *Eur. J. Biochem.*, **247**, 741–753.
6 Been,M.D. (1994) *Trends Biochem. Sci.*, **19**, 251–256.
7 Perrotta,A.T. and Been,M.D. (1991) *Nature*, **350**, 434–436.
8 Suh,Y.A., Kumar,P.K.R., Kawakami,J., Nishikawa,F., Taira,K. and Nishikawa,S. (1993) *FEBS Lett.*, **326**, 158–162.
9 Tanner,N.K., Schaff,S., Thill,G., Petit-Koskas,E., Crain-Denoyelle,A.M. and Westhof,E. (1994) *Curr. Biol.*, **4**, 488–498.
10 Kawakami,J., Yuda,K., Suh,Y.A., Kumar,P.K.R., Nishikawa,F., Maeda,H., Taira,K., Ohtsuka,E. and Nishikawa,S. (1996) *FEBS Lett.*, **394**, 132–136.
11 Lai,Y.C., Lee,J.Y., Liu,H.J., Lin,J.Y. and Wu,H.N. (1996) *Biochemistry*, **35**, 124–131.
12 Jeng,K.S., Daniel,A. and Lai,M.M.C. (1996) *J. Virol.*, **70**, 2403–2410.
13 Fauzi,H., Chiba,A., Nishikawa,F., Roy,M., Kawakami,J. and Nishikawa,S. (1998) *Anal. Chim. Acta*, **365**, 309–317.
14 Branch,A.D. and Robertson,H.D. (1991) *Proc. Natl Acad. Sci. USA*, **88**, 10163–10167.
15 Been,M.D., Perrotta,A.T. and Rosenstein,S.P. (1992) *Biochemistry*, **31**, 11843–11852.
16 Nishikawa,F., Kawakami,J., Chiba,A., Shirai,M., Kumar,P.K.R. and Nishikawa,S. (1996) *Eur. J. Biochem.*, **237**, 712–718.
17 Kawakami,J., Kumar,P.K.R., Suh,Y.A., Nishikawa,F. Kawakami,K., Taira,K. and Nishikawa,S. (1993) *Eur. J. Biochem.*, **217**, 29–36.
18 Nishikawa,F., Fauzi,H. and Nishikawa,S. (1997) *Nucleic Acids Res.*, **25**, 1605–1610.
19 Fauzi,H., Kawakami,J., Nishikawa,F. and Nishikawa,S. (1997) *Nucleic Acids Res.*, **25**, 3124–3130.
20 Wu,H.N. and Huang,Z.S. (1992) *Nucleic Acids Res.*, **20**, 5937–5941.
21 Wu,H.N., Lee,J.Y., Huang,H.W., Huang,Y.S. and Hsueh,T.G. (1993) *Nucleic Acids Res.*, **21**, 4193–4199.
22 Kumar,P.K.R., Suh,Y.A., Taira,K. and Nishikawa,S. (1993) *FASEB J.*, **7**, 124–129.
23 Perrotta,A.T. and Been,M.D. (1996) *Nucleic Acids Res.*, **24**, 1314–1321.
24 Biswas,R., Wahl,M.C., Ban,C. and Sundaralingam,M. (1997) *J. Mol. Biol.*, **267**, 1149–1156.
25 Biswas,R. and Sundaralingam,M. (1997) *J. Mol. Biol.*, **270**, 511–519.
26 Zuker,M. (1989) *Science*, **244**, 48–52.
27 Ananvoranich,S. and Perreault,J.P. (1998) *J. Biol. Chem.*, **273**, 13182–13188.
28 Jeoung,Y.H., Kumar,P.K.R., Suh,Y.A., Taira,K. and Nishikawa,S. (1994) *Nucleic Acids Res.*, **22**, 3722–3727.
29 Kumar,P.K.R., Suh,Y.A., Miyashiro,H., Nishikawa,F., Kawakami,J., Taira,K. and Nishikawa,S. (1992) *Nucleic Acids Res.*, **20**, 3919–3924.
30 Thill,G., Vasseur,M. and Tanner,N.K. (1993) *Biochemistry*, **32**, 4254–4262.
31 Kolk,M.H., Heus,H.A. and Hilbers,C.W. (1997) *EMBO J.*, **16**, 3685–3692.
32 Lynch,S.R. and Tinoco,I.,Jr (1998) *Nucleic Acids Res.*, **26**, 980–987.
33 Bravo,C., Lescure,F., Laugâa,P., Fourrey,J.L. and Favre,A. (1996) *Nucleic Acids Res.*, **24**, 1351–1359.
34 Ferré-D'Amaré,A.R., Zhou,K. and Doudna,J.A. (1998) *Nature*, **395**, 567–574.
35 Makino,S., Chang,M.F., Shieh,C.K., Kamahora,T., Vannier,D., Govindarajan,S. and Lai,M.M.C. (1987) *Nature*, **329**, 343–346.